HHS Public Access

Author manuscript

Circ Arrhythm Electrophysiol. Author manuscript; available in PMC 2016 November 03.

Published in final edited form as:

Circ Arrhythm Electrophysiol. 2015 October ; 8(5): 1122–1132. doi:10.1161/CIRCEP.115.002745.

Identification and Functional Characterization of a Novel *CACNA1C*-Mediated Cardiac Disorder Characterized by Prolonged QT Intervals with Hypertrophic Cardiomyopathy, Congenital Heart Defects, and Sudden Cardiac Death

Nicole J. Boczek, PhD[1,2,3], **Dan Ye, MD**[1], **Fang Jin, MD**[4], **David J. Tester, BS**[1], **April Huseby, BS**[2,4], **J. Martijn Bos, MD, PhD**[1], **Aaron J. Johnson, PhD**[4], **Ronald Kanter, MD**[5,6], and **Michael J. Ackerman, MD, PhD**[1,7]

[1]Department of Molecular Pharmacology & Experimental Therapeutics, Windland Smith Rice Sudden Death Genomics Laboratory

[2]Mayo Graduate School

[3]Center for Clinical & Translational Science

[4]Divison of Immunology & Neurology

[5]Department of Pediatrics & Pediatrics/Cardiology, Duke University School of Medicine, Durham, NC

[6]Miami Children's Hospital, Miami, FL

[7]Departments of Medicine (Division of Cardiovascular Diseases) & Pediatrics (Division of Pediatric Cardiology), Mayo Clinic, Rochester, MN

Abstract

Background—A portion of sudden cardiac deaths (SCD) can be attributed to structural heart diseases such as hypertrophic cardiomyopathy (HCM) or cardiac channelopathies such as long QT syndrome (LQTS); however, the underlying molecular mechanisms are quite distinct. Here, we identify a novel *CACNA1C* missense mutation with mixed loss-of-function/gain-of-function responsible for a complex phenotype of LQTS, HCM, SCD, and congenital heart defects (CHDs).

Methods and Results—Whole exome sequencing (WES) in combination with Ingenuity Variant Analysis was completed on three affected individuals and one unaffected individual from a large pedigree with concomitant LQTS, HCM, and CHDs and identified a novel *CACNA1C* mutation, p.Arg518Cys, as the most likely candidate mutation. Mutational analysis of exon 12 of *CACNA1C* was completed on 5 additional patients with a similar phenotype of LQTS plus a personal or family history of HCM-like phenotypes, and identified two additional pedigrees with mutations at the same position, p.Arg518Cys/His. Whole cell patch clamp technique was used to

Correspondence: Michael J. Ackerman, MD, PhD, Mayo Clinic Windland Smith Rice Sudden Death, Genomics Laboratory, Mayo Clinic, Guggenheim 501, Rochester, MN 55905, Tel: 507-284-0101, Fax: 507-284-3757, ackerman.michael@mayo.edu.

Conflict of Interest Disclosures: Mayo Clinic and MJA receive sales based royalties from Transgenomic's FAMILION-LQTS and FAMILION-CPVT genetic tests

assess the electrophysiological effects of the identified mutations in $Ca_V1.2$, and revealed a complex phenotype, including loss of current density and inactivation in combination with increased window and late current.

Conclusions—Through WES and expanded cohort screening, we identified a novel genetic substrate p.Arg518Cys/His-CACNA1C, in patients with a complex phenotype including LQTS, HCM, and CHDs annotated as cardiac-only Timothy syndrome. Our electrophysiological studies, identification of mutations at the same amino acid position in multiple pedigrees, and co-segregation with disease in these pedigrees provides evidence that p.Arg518Cys/His is the pathogenic substrate for the observed phenotype.

Keywords

L-type calcium channels; long QT syndrome; hypertrophic cardiomyopathy; genetics; sudden cardiac death; Cardiac-only Timothy syndrome

Introduction

Each year, more than 400,000 cases (>1,000 per day) of sudden cardiac death (SCD) are reported in the United States.[1] Many of these deaths can be attributed to coronary artery disease; however, a small portion are caused by inherited structural heart diseases, such as hypertrophic cardiomyopathy (HCM) or structurally normal heart inherited arrhythmia syndromes, such as long QT syndrome (LQTS).[2, 3] Although both HCM and LQTS can cause sudden death due to cardiac arrhythmias, the pathophysiology, disease progression, and underlying molecular/genetic substrates are thought to be distinct.

Largely considered a disorder of the cardiac sarcomere, HCM is defined by cardiac hypertrophy, most commonly of the left ventricle, in the absence of a clinically identifiable etiology, and often presents with fibrosis, myocyte disarray, ventricular septal dysmorphology, coronary artery microvascular disease, and left ventricular outflow tract obstruction.[4, 5] Conversely, LQTS is a disorder of delayed ventricular myocardial repolarization that often manifests as prolongation of the QT interval on an ECG in the setting of a structurally normal heart.[6] Although over 25 HCM-susceptibility genes (mostly encoding for structural proteins)[7] and 17 LQTS-susceptibility genes (encoding for ion channels or channel interacting proteins)[8] have been discovered, a significant number of patients expressing these potentially lethal phenotypes remain genetically elusive.

Here, using next generation pedigree-based whole exome sequencing (WES) on a multi-generational pedigree and a subsequent analysis of additional unrelated patients/pedigrees presenting with a similar cardiac phenotype, we have identified a novel perturbation in the *CACNA1C*-encoded $Ca_V1.2$ calcium channel that confers susceptibility for the concomitant phenotypes of LQTS, HCM, congenital heart defects (CHDs), and SCD that are present in these families.

Methods

Study Subjects

An 11-member (6 affected) multigenerational pedigree presented with a multitude of cardiac signs and symptoms, including marked QT prolongation, HCM, SCD, and CHDs. However, none of the family members had syndactyly, cognitive impairments, facial dysmorphisms, or any other non-cardiac clinical characteristics suggestive of Timothy syndrome (TS). The proband, who was genotype-negative by commercially available LQTS genetic testing, was referred to the Mayo Clinic Windland Smith Rice Sudden Death Genomics Laboratory for further genetic testing. After written consent for this Institutional Review Board-approved study, peripheral blood lymphocytes were obtained from 6 family members. Genomic DNA was obtained using the Puregene DNA Isolation Kit (Qiagen Inc., Valencia, CA). The symptomatic index case, unaffected mother, affected sister, and affected nephew were selected for WES (Figure 1A, cases III.1, II.2, III.4 and IV.1 respectively).

Whole Exome Sequencing

Expanded methods regarding the whole exome sequencing and subsequent bioinformatic analysis are available in the supplemental materials.

CACNA1C Mutational Analysis

Next, we examined our cohort of 37 unrelated patients with clinically robust but genetically elusive LQTS for coexisting echocardiographic evidence of HCM, or family history of HCM-like phenotypes; we found 5 cases with this phenotype (Table 1). These cases were mutation negative after LQTS mutational analysis (by denaturing high performance liquid chromatography and DNA sequencing) of the 3 major LQTS genes: *KCNQ1, KCHN2,* and *SCN5A*, and 8 minor LQTS genes: *AKAP9, ANKB, CAV3, KCNE1, KCNE2, KCNJ2, SCN4B,* and *SNTA1.*

For these 5 unrelated cases with LQTS and concomitant personal or familial HCM, genetic analysis was performed on exon 12 of *CACNA1C* (NM_000719) using polymerase chain reaction and DNA sequencing (ABI Prism 377, Applied Biosystems Inc., Foster City, CA). Primer sequences and PCR conditions are available upon request.

We expanded the pedigrees to include additional blood samples from family members of two of five of these patients to examine exon 12 of *CACNA1C.* All patients and family members signed written consent for this IRB-approved study.

CACNA1C Mammalian Expression Vectors and Site-Directed Mutagenesis

The human wild-type (WT) *CACNA1C* cDNA with an N-terminal enhanced yellow fluorescence protein (EYFP) tag [(EYFP) Nα1c,77] in the pcDNA vector and the cDNA of the *CACNA2D1* gene cloned in pcDNA3.1 vector, and the *CACNB2* cDNA were gifts from Dr. Charles Antzelevitch, Masonic Medical Research Laboratory, Utica NY. The cDNA of *CACNB2b* was subcloned into the bicistronic pIRES2-dsRED2 vector (Clontech, Mountain View, CA). The p.Arg518Cys-CACNA1C and p.Arg518His-CACNA1C missense mutations were engineered into pcDNA3-*CACNA1C*-WT–EYFP vector using primers containing the

missense mutations (available upon request) in combination with the Quikchange II XL Site-Directed Mutagenesis Kit (Stratagene, La Jolla, CA). The integrity of all constructs was verified by DNA sequencing.

HEK293 Cell Culture and Transfection

Expanded methods regarding the HEK293 cell culture and transfection, as well as subsequent electrophysiological measurements, data analysis, and confocal examination of CACNA1C are available in the supplemental materials.

Statistical Analysis

All data points are shown as the mean value and error bars represent the standard error of the mean. Statistics were completed used SigmaPlot 12.0 (San Jose, CA) and GraphPad Prism (La Jolla, CA). Normality was tested by Shapiro-Wilk and constant variance was analyzed for each comparison, and if normality failed, nonparametric methods were utilized. Student's t-test or Mann-Whitney rank sum test was performed to determine statistical significance between two groups, and a $p< 0.05$ was considered significant. One way ANOVA or Kruskal-Wallis in combination with Dunn's method for multiple comparisons was performed to determine statistical significance among our variants versus controls. After correction for multiple comparisons, a $p<0.05$ was considered to be significant.

Results

Multigenerational Pedigree with LQTS, HCM, SCD, and CHDs

The index case is a 33-year-old female (III.1, Figure 1A; Table 2) who presented at 25 years of age with QT prolongation during pregnancy. Subsequent medical history revealed a ventricular septal defect (VSD) and a family history of SCD. Her ECG exhibited a QTc of 500 ms, first degree AV block, and her medical therapy included the placement of an implantable cardioverter defibrillator (ICD). She later experienced peripartum cardiomyopathy after giving birth to triplets. Several years later, she had an abnormal echocardiogram with ventricular septal hypertrophy with a maximum septal wall thickness of 15 mm.

After reviewing her family history (Table 2), it was identified that her father (II.1) died at 36 years-of-age due to a cardiac arrhythmia secondary to HCM with cardiac hypertrophy and fibrosis noted at autopsy. Her brother (III.2) died at 24 years-of-age, when first responders found him in ventricular fibrillation and were unable to resuscitate him. His autopsy also revealed underlying HCM with cardiomegaly and interstitial fibrosis. An ECG performed 2 years prior to his death revealed QT prolongation with a QTc of 490 ms. Her deceased brother's son (IV.1) has marked QT prolongation (QTc, 522 ms) and has been treated with an ICD. Her living brother (III.3) has normal QTc values. Her sister's (III.4) ECGs showed QT prolongation with a QTc of 491 ms.

Overall, the family history is unique and atypical, with overt QT prolongation presenting in some cases and cardiomyopathies including HCM, with or without CHDs, in an autosomal dominant inheritance pattern. However, none of the patients have extra-cardiac phenotypes,

such as those observed in Timothy syndrome (TS). Taken altogether, the phenotypic sequela is representative of an autosomal dominant condition, with features consistent with cardiac only Timothy syndrome (COTS).

WES for Novel Pathogenic Substrate Identification in a Large Multigenerational Pedigree

Utilizing WES, we genetically interrogated our index case (III.1), her affected sister (III.4), affected nephew (IV.1), and unaffected mother (II.2). Overall, 146,020 variants were identified (Figure 1B). Utilizing Ingenuity Variant Analysis, we were able to filter our total number of plausible candidate variants to 29 (Figure 1B). Utilizing genes that have been associated previously with LQTS, cardiomyopathy, SCD, and diseases consistent with these phenotypes, we identified one novel, ultra-rare variant, c.1552C>T in exon 12 of the *CACNA1C* encoded $Ca_V1.2$ L-type calcium channel (LTCC), which leads to an arginine to cysteine change at amino acid position 518 (p.Arg518Cys) in the I-II cytoplasmic linker of $Ca_V1.2$ (Figure 2).

Follow-Up Cohort Analysis

Based on the unique and novel phenotype identified within this pedigree, we examined our cohort of 37 unrelated patients with clinically robust but genetically elusive LQTS for cases with a personal or family history of phenotypes suggestive of HCM, and a total of 5 patients met those criteria (Table 1). Using PCR amplification and Sanger-based DNA sequencing, we interrogated exon 12 of *CACNA1C*. Interestingly, 2/5 (40%) had a variant in exon 12, both at the 518^{th} amino acid, one encoding for arginine to cysteine (p.Arg518Cys), like our original pedigree, and the second encoding for arginine to histidine (p.Arg518His).

The index case (II.1) in pedigree 2 was diagnosed with LQTS with a QTc of 480 ms after a screening ECG was performed because of his father's (I.2) diagnosis of HCM. (Table 2; Figure 3, Pedigree 2). The index case (III.1) in pedigree 3 was diagnosed with LQTS with a QTc of 500 ms. She was born with a cleft mitral valve and had surgical repair of an atrial septal defect (ASD) at 19 months. During an unrelated hernia repair, she had intraoperative torsades des pointes for 5-10 beats and was implanted subsequently with an ICD. Her sister (III.2) was diagnosed with obstructive HCM at a young age, and she had two myectomies before the age of 5. She also had QT prolongation which at the time was attributed to her HCM. She died suddenly and unexpectedly at 30 years of age, and her autopsy reported symmetrical hypertrophy, and fibrosis; cause of death was likely due to arrhythmia. Her mother (II.1) has an enlarged septum and QT prolongation, and she has a pacemaker. Her maternal aunt (II.2) and maternal cousin (III.3) have been diagnosed with HCM. Family member III.3 had subaortic stenosis, had a left ventricular septal myectomy, has a history of supraventricular tachycardia and first degree AV block, and has been treated with verapamil. Her maternal grandfather (I.1) died suddenly and unexpectedly in the hospital at 64 years-of-age (Table 2; Figure 3, Pedigree 3). Genetic interrogation using PCR and Sanger-based DNA sequencing of exon 12 of *CACNA1C* in family members in all three pedigrees revealed that p.Arg518Cys/His co-segregated with the abnormal cardiac phenotypes (Figure 3).

In Vitro Functional Analysis of p.Arg518Cys/His-CACNA1C

To better understand the effect that p.Arg518Cys/His has on the $Ca_V1.2$ channel, we utilized whole cell patch clamp technique to determine whether there are electrophysiological differences between these mutants and WT-$Ca_V1.2$ channels in HEK293 cells. Typical I_{Ca} tracings of voltage-dependent activation from WT and p.Arg518Cys/His are shown in Figure 4A. Analysis of the current-voltage relationship shows that p.Arg518Cys/His mutants dramatically decrease I_{Ca} current density from −10 mV to +70 mV ($p<0.05$ vs. WT, Figure 4B). The peak current density was reduced by 55.6% and 63.2% respectively from −69.3 ± 7.0 pA/pF (WT, n=15) to −30.8 ± 5.2 pA/pF (p.Arg518Cys, n=14; $p<0.0001$) and to −25.5 ± 5.8 pA/pF (p.Arg518His, n=15; $p<0.0001$, Figure 4C).

Due to the reduction of current density observed with the p.Arg518Cys/His variants, we utilized the EYFP-tag on CACNA1C to examine the localization of mutant and WT-$Ca_V1.2$ proteins. Visual comparison highlights a centralized punctate pattern of fluorescence with p.Arg518Cys, which is not observed in WT cells (Figure 4D). Using the confocal microscopy images, we compared the peripheral (membrane):central (cytosol) ratio between WT and p.Arg518Cys. We found that WT had a ratio of 0.97 ± 0.05 (n=10), whereas p.Arg518Cys had a ratio of 0.81 ± 0.04 (n=10; p=0.02; Figure 4E), suggesting that less mutant channels are localized to the membrane and that p.Arg518Cys may affect trafficking.

Typical tracings of steady-state inactivation for WT and p.Arg518Cys/His are shown in Figure 5A. Steady-state inactivation was assessed by a standard 2 pulse voltage-clamp protocol (see inset Figure 5A and figure legend). A plot of the inactivation curves shows that p.Arg518Cys and p.Arg518His shifted $V_{1/2}$ of inactivation to more depolarized potentials by +6.8 mV and +7.0 mV respectively from −20.9 ± 0.4 mV (WT, n=15) to −14.1 ± 0.5 (Arg518Cys, n=14, $p<0.001$) and to −13.9 ± 0.7 mV (p.Arg518His, n=15, $p<0.001$; Figure 5B). The respective k (slope factor) showed a significant difference between the mutants and WT from 5.6 ± 0.2 (WT, n=15) to 8.2 ± 0.4 (p.Arg518Cys, n=14, $p<0.001$) and to 8.6 ± 0.6 (p.Arg518His, n=15, $p<0.001$). A plot of the activation curves shows that the p.Arg518His mutation shifted $V_{1/2}$ of activation to a more depolarized potential by +4.5 mV from +13.4 ± 1.1 mV (WT, n=15) to +17.9 ± 0.8 mV (p.Arg518His, n=15, $p = 0.004$; Figure 5B). However, p.Arg518Cys did not significantly shift activation. In addition, the respective k (slope factor) showed no significant difference between the groups: 6.9 ± 0.4 (WT, n=15), 7.7 ± 0.4 (p.Arg518Cys, n=14), 8.0 ± 0.4 (p.Arg518His, n=15). When voltage-dependent activation and steady-state inactivation are plotted together, large increases in the window current can be observed (Figure 5B).

I_{Ca} decay after 90% of peak was best fit by two exponentials with two τ values representing fast and slow inactivation. From +40 to +50, p.Arg518Cys/His revealed slower inactivation τ in the fast component of decay time (corrected $p < 0.05$, Figure 5C). From +20 to +50 mV, p.Arg518Cys/His revealed a slower inactivation τ in the slow component of the decay time (corrected $p < 0.05$, Figure 5D).

Finally, we examined late current of I_{CaL}; the typical traces can be seen in Figure 5E. In addition, we normalized late current to the peak current, and compared the percent of each group, and the mutations conferred an increased late current by 7.0 fold and 6.6 fold

respectively from 2.6% ± 0.5 (WT, n=15) to 20.9% ± 2.5 (p.Arg518Cys, n=14, p<0.001) and to 19.7% ± 1.9 (p.Arg518His, n=15, p<0.001; Figure 5F).

In Vitro Functional Analysis of p.Arg518Cys-CACNA1C with or without $BaCl_2$ perfusion

I_{Ca} CACNA1C-WT and p.Arg518Cys reached peak at +30 mV, whereas I_{Ba} CACNA1C-WT and p.Arg518Cys reached peak at +10 mV. Both WT and p.Arg518Cys mutant displayed robust I_{Ba} currents at +10 mV compared with I_{Ca} currents. The p.Arg518Cys mutation exhibited slower inactivation kinetics than WT under both $CaCl_2$ and $BaCl_2$ perfusion. Typical $Ca_V1.2$ CACNA1C-WT and p.Arg518Cys I_{Ca} and I_{Ba} tracings of voltage-dependent activation at +10 mV and +30 mV are shown in Figure 6A. Voltage-dependent inactivation (VDI) was presented as fraction of current remaining after 500 ms depolarization normalized to peak current (r_{500}) across various voltages. The extent of Ca^{2+}-dependent inactivation (CDI) was calculated as $f_{500}= (r_{500/Ba}-r_{500/Ca})/r_{500/Ba.}$ The p.Arg518Cys mutation significantly decelerated VDI from +10 mV to +30 mV under both $BaCl_2$ and $CaCl_2$ perfusion (Figure 6B). However, p.Arg518Cys did not change CDI of $Ca_V1.2$ channel at +30 mV significantly with f_{500} = 0.62 ± 0.07 (p.Arg518Cys, n = 5) compared to f_{500} = 0.55 ± 0.09 (WT, n = 5).

Discussion

Familial WES is a powerful tool for identifying the underlying genetic substrate in novel disorders. In this study, we identified a pedigree with multiple cardiac abnormalities, including LQTS, HCM, CHDs, and SCD. WES of three affected and one unaffected family member in combination with Ingenuity Variant Analysis suggested a novel mutation p.Arg518Cys-CACNA1C as the probable pathogenic substrate for the COTS phenotype observed in this pedigree. Follow-up cohort analysis revealed two additional pedigrees, with very similar phenotypes, having mutations at the exact same amino acid position (p.Arg518Cys and p.Arg518His).

CACNA1C encodes for the α-subunit of the $Ca_V1.2$ LTCC, which is critical for the plateau phase of the cardiac action potential, cellular excitability, excitation-contraction coupling, and regulation of gene expression.[20, 21] Perturbations of *CACNA1C* have been associated with several different cardiac arrhythmia disorders, which can be differentiated into two groups, loss-of-function CACNA1C–mediated disease leading to Brugada syndrome (BrS),[9] and gain-of-function CACNA1C–mediated disease leading to either Timothy syndrome (TS)[10] or LQTS.[11]

Of the gain-of-function CACNA1C-mediated diseases, TS, is an extremely rare, sporadic disorder, characterized by a myriad of multisystem abnormalities, including a cardiac phenotype of QT prolongation, HCM, CHDs, premature SCD and an extra-cardiac phenotype of syndactyly, facial dysmorphisms, and neurological symptoms including autism and intellectual disability.[22] Although it was speculated initially that gain-of-function mutations within *CACAN1C* would lead to this complex multisystem phenotype of TS, *CACNA1C* mutations were described recently in cases of pure congenital LQTS devoid of other cardiac or other organ system abnormalities.[11] Conversely, concomitant QT-prolongation is common in patients with HCM, although the exact pathophysiology of this

electrocardiographic finding remains unclear.[23] Interestingly, the pedigrees identified within this study seem to have a phenotype that lies between TS and LQTS, representing a "cardiac-only" TS (COTS) phenotype of LQTS, HCM, CHDs, and SCD. Akin to patients with CACNA1C-mediated LQTS, none of the individuals within the three pedigrees have any of the extra-cardiac phenotypes associated with TS.

In order to confirm the disease-causing nature of the p.Arg518Cys/His mutations and to attempt to better understand the resultant COTS phenotype, heterologous expression of the $Ca_V1.2$ was used to elucidate the functional perturbation of p.Arg518Cys/His. Interestingly, unlike the previously reported LQTS-associated mutations which produced an overall gain of current density,[11, 12] p.Arg518Cys/His led to an overall loss of current density by ~59%. Confocal imaging provided evidence that there was a higher proportion of CACNA1C mutant channels in the center versus the periphery of the cell, highlighting the possibility of a trafficking defect, which may explain the overall reduction in current density. The p.Arg518Cys/His variant lies within the I-II linker of CACNA1C, and within this linker is the AID (α-interaction domain), in which the β-subunit binds (Figure 2). Although p.Arg518Cys/His does not fall within the AID, the β-subunit is known to aid in α-subunit trafficking and regulation of channel kinetics,[24,25] therefore one could hypothesize that the p.Arg518Cys/His may disrupt folding of the I-II linker, altering the normal interaction between the AID and β-subunit, leading to significant changes in trafficking and channel kinetics.

In addition, p.Arg518Cys/His also caused a gain-of-function shift in the inactivation curves to more depolarized potentials, leading to a significant increase in the window current. Increases in window current, due to gain-of-function shifts in *activation* were identified recently in p.Ile1166Thr-CACNA1C, a mutation attributed to TS.[13] Finally, p.Arg518Cys/His elicited a ~7 fold increase in the overall late current due to slower inactivation of $Ca_V1.2$ mutant channels, and led to decelerating VDI. Similarly, the original TS-mutations p.Gly406Arg and p.Gly402Ser (also in the I-II linker) lead to almost complete loss of inactivation of $Ca_V1.2$ and alterations in VDI.[10, 14, 26]

Although a mixed phenotype including loss of current density in combination with an increased window current and loss of inactivation was shown, we believe that the p.Arg518Cys/His mutations are capable of producing prolonged QT intervals. Modeling studies of the TS-associated mutations, p.Gly406Arg[10] and p.Ile1166Thr,[13] with the electrophysiological phenotypes including loss of inactivation and increased window current with loss of current density, respectively, have shown action potential prolongation and spontaneous delayed afterdepolarizations (DADs; p.Gly406Arg) or early afterdepolarizations (EADs; p.Ilell66Thr). Both DADs and EADs are capable of leading to ventricular fibrillation and sudden death. The modeling studies completed on p.Gly406Arg were further validated in induced pluripotent stem cell (iPSC) models, in which prolonged action potentials were observed.[27] The similarities in the electrophysiological phenotypes of our identified variants and those previously described in TS provides evidence that the p.Arg518Cys/His mutations can cause action potential prolongation at the myocyte level and QT prolongation clinically.

However, it is less well understood why these mutations would lead to a HCM phenotype or CHDs, as observed in our pedigrees. Interestingly, TS has clinical manifestations including HCM and CHDs. In fact, as many as 61% of TS cases have some form of CHDs including HCM;[22] therefore, it may not be that surprising that the patients within our identified pedigrees similarly manifest with cardiac hypertrophy and CHDs including VSD and ASD.

The exact pathophysiology of HCM and CHDs in TS is yet to be established. However, it has been suggested previously that protein expression in pathways regulating Ca^{2+} within cardiac tissue may be perturbed in patients with CHDs and may result in hypertrophy.[28] Those studies, in combination with what has been observed in our pedigrees and TS, suggest that proper regulation of Ca^{2+} and potentially the LTCC are crucial for cardiac development, and perturbation of Ca^{2+} handling could lead to developmental abnormalities leading to CHDs.

Abnormal calcium handling has also been described in various models of cardiac hypertrophy. What has been unclear in the past is whether this Ca^{2+} irregularity is secondary to hypertrophy or related to the primary pathogenesis of disease.[29] Recently, Lan and colleagues examined Ca^{2+} handling in an iPSC model of HCM and found irregular Ca^{2+} transients and elevated diastolic $[Ca^{2+}]_i$ before overt phenotypic expression of cardiac hypertrophy as seen in HCM. This finding, in combination with their finding that LTCC blockers, such as verapamil, mitigated cellular hypertrophy, suggest that dysregulation of Ca^{2+} may be a central mechanism for disease development.[30] The phenotypes observed within our pedigrees also support the findings of Lan and colleagues, suggesting that Ca^{2+} handling could be a primary cause for hypertrophy. As shown in our electrophysiological studies, the p.Arg518Cys/His leads to Ca^{2+} mishandling, through constitutively active LTCC, and over time, many of the patients within the pedigrees who are mutation positive acquire left ventricular hypertrophy.

CACNA1C-Mediated Clinical Phenotypes

A large paradox emerges in the context of *CACNA1C* mutations in the human heart as to why some gain-of-function mutations cause a multiple organ-system phenotype like TS, some a LQTS-only phenotype, and some a cardiac-only TS (COTS) phenotype such as the one described within this study. Initially, analyzing electrophysiological phenotypes of each of these diseases as described above, it was easy to distinguish CACNA1C-mediated LQTS. Based on our original findings, the major electrophysiological phenotype of CACNA1C-associated LQTS was marked gain in $Ca_V1.2$ current density,[11] whereas TS[10,20] and p.Arg518Cys/His alter the kinetic properties of the channel. It also seemed as if TS-associated mutations localized to specific channel regions, at the S6/interdomain linker boundaries,[13] whereas the COTS- and LQTS- associated mutations primarily localize to intracellular linker loops, and the N-and C-terminus (Figure 2). Therefore, it could have been hypothesized that the mechanism for pure LQTS is largely due to location and the electrophysiological perturbation caused by the mutation.

However, since the initial discovery of CACNA1C-mediated LQTS, the spectrum and prevalence of mutations within CACNA1C has expanded greatly. Two novel case reports identified the previously TS-associated p.Gly402Ser mutation in patients without the

neurological phenotypes associated with TS, rather these patients presented primarily with QT prolongation and ventricular fibrillation. In addition, these case reports suggest that the neurological phenotype observed with p.Gly402Ser may stem from the cardiac insults that had taken place early in development, rather than be due to the p.Gly402Ser mutation itself. [15, 16] In a similar fashion, Wemhoner and colleagues found an individual with phenotypes consistent with TS with a p.Ile1166Thr mutation,[17] matching previous reports.[13] However, they found a second mutation, p.Ile1166Val in a patient exhibiting a LQTS-only phenotype. Although the electrophysiological characteristics between p.Ile1166Thr and p.Ile1166Val were distinct, this finding, along with the novel case reports surrounding p.Gly402Ser, begin to highlight that mutation location may not be the final determinant of disease manifestation.

After the identification of more CACNA1C mutations in LQTS and TS, a more comprehensive comparison of the electrophysiological characteristics could be made. Taken altogether, there are LQTS-associated mutations that present with only increases in peak current density (p.Pro857Arg, p.Ilell66Val), there are mutations that affect only channel kinetics (p.Arg860Gly, p.Ile1475Met, p.Glu1496Lys), and there are mutations that affect both (p.Ala28Thr, p.Ala582Asp, p.Arg858His). In addition to our CACNA1C-mediated LQTS, we have TS mutations (p.Gly406Arg exon 8/8A, p.Gly402Ser exon 8, p.Ile1166Thr) that affect kinetics and in some cases current density. And finally, we have the COTS-associated mutations (p.Arg518Cys/His), that affect both current density and channel kinetics. Therefore, these variants cannot easily be separated by the electrophysiological characteristics.

Collectively, it seems as if the disease phenotypes observed with mutations in the calcium channel are more complex than the location of the mutation within the channel and the underlying electrophysiological perturbations that the particular mutation causes. There are several different unexplored explanations that may determine the disease pathogenesis. It may be possible that the amino acid change itself, for instance p.Ile1166Thr causes TS, whereas p.Ile1166Val causes LQTS, confers disease phenotype. It is also possible that the binding of partner proteins leading to complex signaling cascades may also be important to disease manifestation. For example, Krey and colleagues found that the location of the p.Gly406Arg mutation may be critical for the neurological phenotypes seen in TS. The p.Gly406Arg mutation leads to more dendritic retraction than WT cells regardless of the presence of pore mutations eliminating Ca^{2+} influx, highlighting the independence of this function from proper $Ca_V1.2$ electrophysiology. They identified that p.Gly406Arg mutation disrupted binding between Gem and $Ca_V1.2$, altering signaling cascades regulated by Gem and RhoA, providing evidence that this interaction is essential to prevent dendritic retraction, and highlighting that binding partners and signaling cascades may be critical for disease presentation.[31] Finally, it also may be possible that there are other genetic or epigenetic factors may play a role in the disease pathogenesis causing different CACNA1C mutations to lead to different phenotypic manifestations in each patient.

Only one conclusion can be made for certain; there definitely are regions within CACNA1C that seem to resemble genetic “hotspots” which lead to cardiac disease. The S6/interdomain linker loop regions are capable of leading to severe LQTS or TS phenotypes,

p.Arg518Cys/His lead to a COTS phenotype, the II-III linker has a multitude of LQTS-associated CACNA1C mutations. Future studies will be necessary to unravel the differences between these mutations, and why, despite their location and electrophysiological similarities, these regions are capable of producing distinct clinical phenotypes ranging the spectrum of TS, COTS, and LQTS.

Conclusions

Through WES and expanded cohort screening, we identified a novel genetic substrate, p.Arg518Cys/His-CACNA1C, in patients with a complex phenotype including LQTS, HCM, CHDs, and SCD here referred to as cardiac-only Timothy syndrome (COTS). Our electrophysiological studies identified a complex phenotype, including loss of current density in combination with increased window current and late current, and decelerating VDI. Based on the functional studies, the identification of mutations at the same amino acid position, and co-segregation with disease in three different pedigrees, these two novel, ultra-rare missense mutations, p.Arg518Cys and p.Arg518His, cause COTS.

Supplementary Material

Refer to Web version on PubMed Central for supplementary material.

Acknowledgments

Funding Sources: This work was supported by the Windland Smith Rice Comprehensive Sudden Cardiac Death Program (M.J.A.), the Dr. Scholl Foundation (M.J.A), Hannah Wernke Memorial Foundation (M.J.A), the Sheikh Zayed Saif Mohammed Al Nahyan Fund in Pediatric Cardiology Research (M.J.A.). N.J.B was supported by CTSA Grant (ULI TR000135) from the National Center for Advancing Translational Science, a component of the National Institutes of Health.

References

1. Go AS, Mozaffarian D, Roger VL, Benjamin EJ, Berry JD, Blaha MJ, Dai S, Ford ES, Fox CS, Franco S, Fullerton HJ, Gillespie C, Hailpern SM, Heit JA, Howard VJ, Huffman MD, Judd SE, Kissela BM, Kittner SJ, Lackland DT, Lichtman JH, Lisabeth LD, Mackey RH, Magid DJ, Marcus GM, Marelli A, Matchar DB, McGuire DK, Mohler ER 3rd, Moy CS, Mussolino ME, Neumar RW, Nichol G, Pandey DK, Paynter NP, Reeves MJ, Sorlie PD, Stein J, Towfighi A, Turan TN, Virani SS, Wong ND, Woo D, Turner MB. Executive summary: Heart disease and stroke statistics--2014 update: A report from the American Heart Association. Circulation. 2014; 129:399–410. [PubMed: 24446411]
2. Chugh SS, Reinier K, Teodorescu C, Evanado A, Kehr E, Al Samara M, Mariani R, Gunson K, Jui J. Epidemiology of sudden cardiac death: clinical and research implications. Prog Cardiovasc Dis. 2008; 51:213–228. [PubMed: 19026856]
3. Boczek NJ, Tester DJ, Ackerman MJ. The molecular autopsy: An indispensable step following sudden cardiac death in the young? Herzschrittmacherth Elektrophysiol. 2012; 23:167–173.
4. Maron BJ. Hypertrophic cardiomyopathy: a systematic review. JAMA. 2002; 287:1308–1320. [PubMed: 11886323]
5. Maron BJ, Towbin JA, Thiene G, Antzelevitch C, Corrado D, Arnett D, Moss AJ, Seidman CE, Young JB. Contemporary definitions and classification of the cardiomyopathies: An American Heart Association scientific statement from the Council on Clinical Cardiology, Heart Failure and Transplantation Committee; Quality of Care and Outcomes Research and Functional Genomics and Translational Biology Interdisciplinary Working Groups; and Council on Epidemiology and Prevention. Circulation. 2006; 113:1807–1816. [PubMed: 16567565]

6. Schwartz PJ, Ackerman MJ. The long QT syndrome: A transatlantic clinical approach to diagnosis and therapy. Eur Heart J. 2013; 34:3109–3116. [PubMed: 23509228]
7. Roma-Rodrigues C, Fernandes AR. Genetics of hypertrophic cardiomyopathy: advances and pitfalls in molecular diagnosis and therapy. Appl Clin Genet. 2014; 7:195–208. [PubMed: 25328416]
8. Giudicessi JR, Ackerman MJ. Genotype- and phenotype-guided management of congenital long QT syndrome. Curr Probl Cardiol. 2013; 38:417–455. [PubMed: 24093767]
9. Burashnikov E, Pfeiffer R, Barajas-Martinez H, Delpón E, Hu D, Desai M, Borggrefe M, Häissaguerre M, Kanter R, Pollevick GD, Guerchicoff A, Laiño R, Marieb M, Nademanee K, Nam G-B, Robles R, Schimpf R, Stapleton DD, Viskin S, Winters S, Wolpert C, Zimmern S, Veltmann C, Antzelevitch C. Mutations in the cardiac L-type calcium channel associated with inherited J-wave syndromes and sudden cardiac death. Heart Rhythm. 2010; 7:1872–1882. [PubMed: 20817017]
10. Splawski I, Timothy KW, Sharpe LM, Decher N, Kumar P, Bloise R, Napolitano C, Schwartz PJ, Joseph RM, Condouris K, Tager-Flusberg H, Priori SG, Sanguinetti MC, Keating MT. Ca(v)1.2 calcium channel dysfunction causes a multisystem disorder including arrhythmia and autism. Cell. 2004; 119:19–31. [PubMed: 15454078]
11. Boczek NJ, Best JM, Tester DJ, Giudicessi JR, Middha S, Evans JM, Kamp TJ, Ackerman MJ. Exome sequencing and systems biology converge to identify novel mutations in the L-type calcium channel, cacna1c, linked to autosomal dominant long QT syndrome. Circ Cardiovasc Genet. 2013; 6:279–289. [PubMed: 23677916]
12. Fukuyama M, Wang Q, Kato K, Ohno S, Ding WG, Toyoda F, Itoh H, Kimura H, Makiyama T, Ito M, Matsuura H, Horie M. Long QT syndrome type 8: Novel CACNA1C mutations causing QT prolongation and variant phenotypes. Europace. 2014; 16:1828–1837. [PubMed: 24728418]
13. Boczek NJ, Miller EM, Ye D, Nesterenko VV, Tester DJ, Antzelevitch C, Czosek RJ, Ackerman MJ, Ware SM. Novel Timothy syndrome mutation leading to increase in CACNA1C window current. Heart Rhythm. 2015; 12:211–219. [PubMed: 25260352]
14. Splawski I, Timothy KW, Decher N, Kumar P, Sachse FB, Beggs AH, Sanguinetti MC, Keating MT. Severe arrhythmia disorder caused by cardiac L-type calcium channel mutations. Proc Natl Acad Sci U S A. 2005; 102:8089–8096. [PubMed: 15863612]
15. Hiippala A, Tallila J, Myllykangas S, Koskenvuo J, Alastalo T. Expanding the phenotype of Timothy syndrome type 2: An adolescent with ventricular fibrillation but normal development. Am J Med Genet A. 2015; 167A:629–634. [PubMed: 25691416]
16. Frohler S, Kieslich M, Langnick C, Feldkamp M, Opgen-Rhein B, Berger F, Will J, Chen W. Exome sequencing helped the fine diagnosis of two siblings afflicted with atypical Timothy syndrome (TS2). BMC Med Genet. 2014; 15:48. [PubMed: 24773605]
17. Wemhoner K, Friedric C, Stallmeyer B, Coffey A, Grace A, Zumhagen S, Seebohm G, Ortiz-Bonnin B, Rinne S, Sachse F, Schulze-Bahr E, Decher N. Gain-of-function mutations in the calcium channel CACNA1C (Cav1.2) cause non-syndromic long-QT but not Timothy syndrome. J Mol Cell Cardiol. 2014; 80:186–195.
18. Antzelevitch C, Pollevick GD, Cordeiro JM, Casis O, Sanguinetti MC, Aizawa Y, Guerchicoff A, Pfeiffer R, Oliva A, Wollnik B, Gelber P, Bonaros EP Jr. Burashnikov E, Wu Y, Sargent JD, Schickel S, Oberheiden R, Bhatia A, Hsu LF, Haissaguerre M, Schimpf R, Borggrefe M, Wolpert C. Loss-of-function mutations in the cardiac calcium channel underlie a new clinical entity characterized by ST-segment elevation, short QT intervals, and sudden cardiac death. Circulation. 2007; 115:442–449. [PubMed: 17224476]
19. Gillis J, Burashnikov E, Antzelevitch C, Blaser S, Gross G, Turner L, Babul-Hirji R, Chitayat D. Long QT, syndactyly, joint contractures, stroke and novel CACNA1C mutation: Expanding the spectrum of timothy syndrome. Am J Med Genet A. 2012; 158A:182–187. [PubMed: 22106044]
20. Benitah JP, Alvarez JL, Gomez AM. L-type ca2+ current in ventricular cardiomyocytes. J Mol Cell Cardiol. 2010; 48:26–36. [PubMed: 19660468]
21. Dai S, Hall DD, Hell JW. Supramolecular assemblies and localized regulation of voltage-gated ion channels. Physiol Rev. 2009; 89:411–452. [PubMed: 19342611]
22. NCBI: Books: GeneReviews. Timothy Syndrome. National Center for Biotechnology Information; web site. www.ncbi.nlm.nih.gov/books/NBK1403. [December 15, 2014]

23. Johnson JN, Grifoni C, Bos JM, Saber-Ayad M, Ommen SR, Nistri S, Cecchi F, Olivotto I, Ackerman MJ. Prevalence and clinical correlates of QT prolongation in patients with hypertrophic cardiomyopathy. Eur Heart J. 2011; 32:1114–1120. [PubMed: 21345853]
24. Van Petegem F, Clark K, Chatelain F, Minor D. Structure of a complex between voltage-gated calcium channel beta-subunit and alpha-subunit domain. Nature. 2004; 429:671–675. [PubMed: 15141227]
25. Almagor L, Chomsky-Hecht O, Ben-Mocha A, Hendin-Barak D, Dascal N, Hirsch J. The role of a voltage-dependent Ca2+ channel intracellular linker: A structure-function analysis. J Neurosci. 2012; 32:7602–7613. [PubMed: 22649239]
26. Almagor L, Chomsky-Hecht O, Ben-Mocha A, Hendin-Barak D, Dascal N, Hirsch JA. Cav1.2 I-II linker structure and Timothy syndrome. Channels. 2012; 6:468–472. [PubMed: 22990809]
27. Yazawa M, Hsueh B, Jia X, Pasca AM, Bernstein JA, Hallmayer J, Dolmetsch RE. Using induced pluripotent stem cells to investigate cardiac phenotypes in Timothy syndrome. Nature. 2011; 471:230–234. [PubMed: 21307850]
28. Wu Y, Feng W, Zhang H, Li S, Wang DW, Pan X, Hu S. Ca2+-regulatory proteins in cardiomyocytes from the right ventricle in children with congenital heart disease. J Transl Med. 2012; 10:67. [PubMed: 22472319]
29. Han L, Li Y, Tchao J, Kaplan AD, Lin B, Mich-Basso J, Lis A, Hassan N, London B, Bett GC, Tobita K, Rasmusson RL, Yang L. Study familial hypertrophic cardiomyopathy using patient-specific induced pluripotent stem cells. Cardiovasc Res. 2014; 104:258–269. [PubMed: 25209314]
30. Lan F, Lee AS, Liang P, Sanchez-Freire V, Nguyen PK, Wang L, Han L, Yen M, Wang Y, Sun N, Abilez OJ, Hu S, Ebert AD, Navarrete EG, Simmons CS, Wheeler M, Pruitt B, Lewis R, Yamaguchi Y, Ashley EA, Bers DM, Robbins RC, Longaker MT, Wu JC. Abnormal calcium handling properties underlie familial hypertrophic cardiomyopathy pathology in patient-specific induced pluripotent stem cells. Cell Stem Cell. 2013; 12:101–113. [PubMed: 23290139]
31. Krey JF, Pasca SP, Shcheglovitov A, Yazawa M, Schwemberger R, Rasmusson R, Dolmetsch RE. Timothy syndrome is associated with activity-dependent dendritic retraction in rodent and human neurons. Nat Neurosci. 2013; 16:201–209. [PubMed: 23313911]

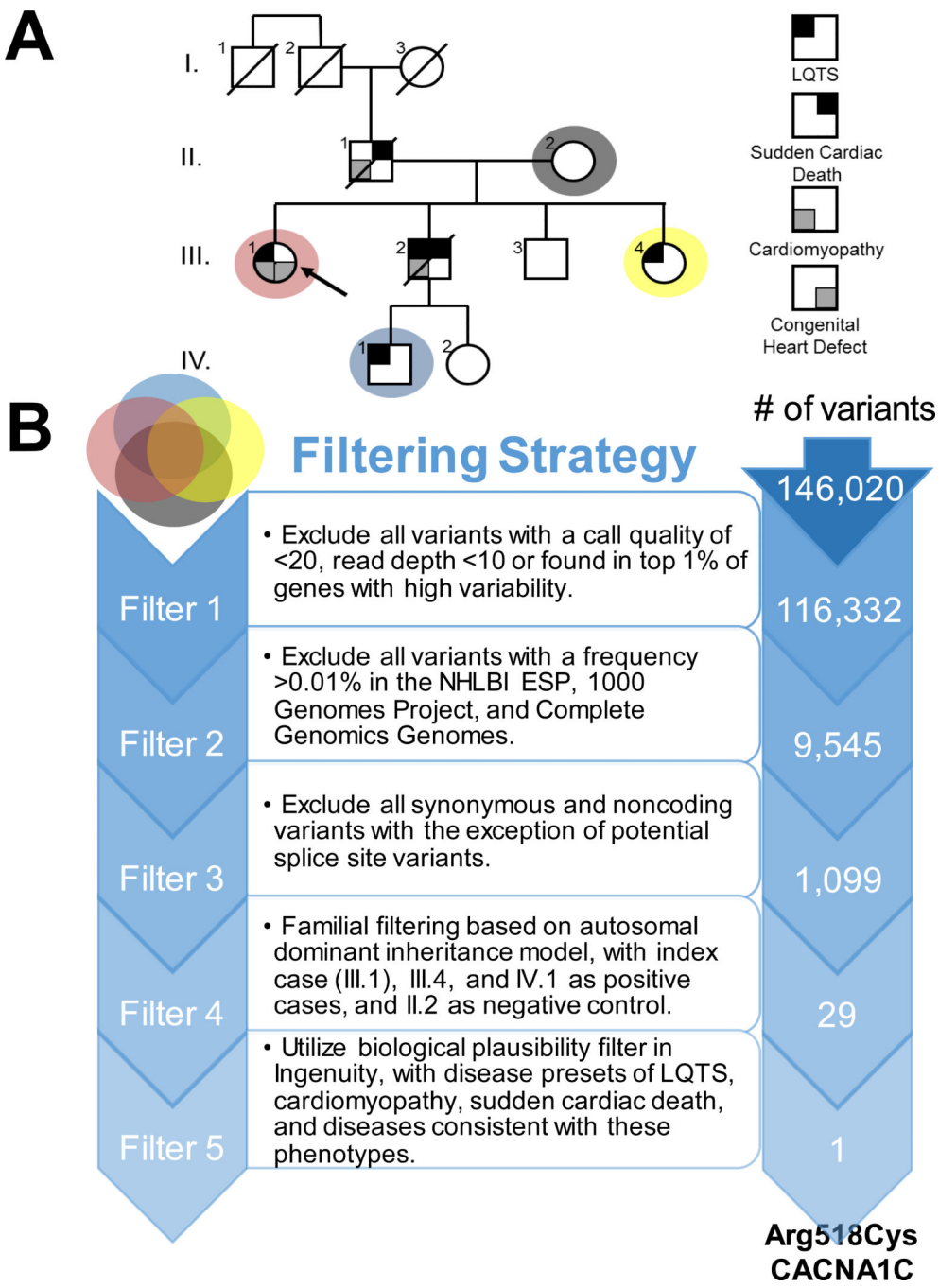

Figure 1.

Pedigree and WES Filtering Strategy. **(A)** Pedigree with LQTS, SCD, cardiomyopathy, and CHDs (see key to right) that was utilized for WES. Individuals who underwent WES are highlighted with grey, red, yellow, and blue circles. **(B)** The filtering strategy utilized on this pedigree, showing the number of variants eliminated at each step.

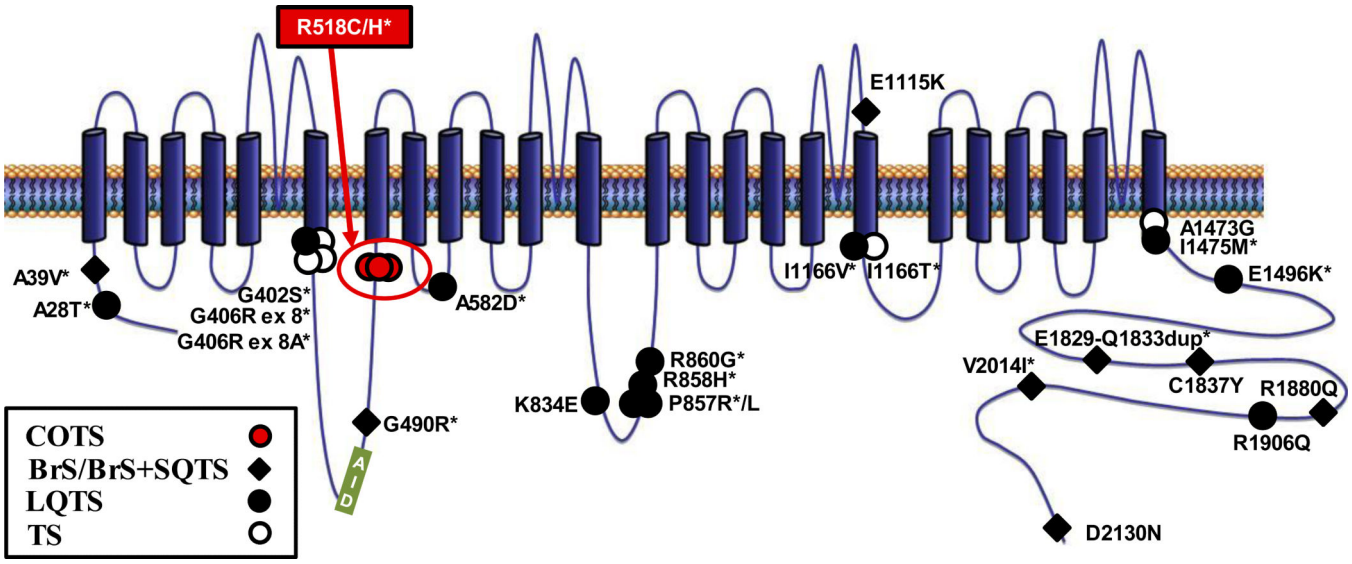

Figure 2.

Topology of CACNA1C. Shown is the topology of *CACNA1C*-encoded $Ca_V1.2$ in the membrane. The location of the p.Arg518Cys/His mutations, associated with cardiac-only Timothy syndrome, as identified in the pedigrees, are highlighted in red circles. In addition, other published CACNA1C mutations in Brugada syndrome (BrS)/Brugada syndrome + short QT syndrome (BrS+SQTS; black diamonds),[9, 18] long QT syndrome (LQTS; black circles),[11, 12, 15-17] and Timothy syndrome (TS; white circles),[10, 13-16, 19] are highlighted. Shown in green is the AID (α-interaction domain; amino acids 428-445), the domain in which the β-subunit is known to bind. Variants with asterisks represent those that have been functionally characterized.

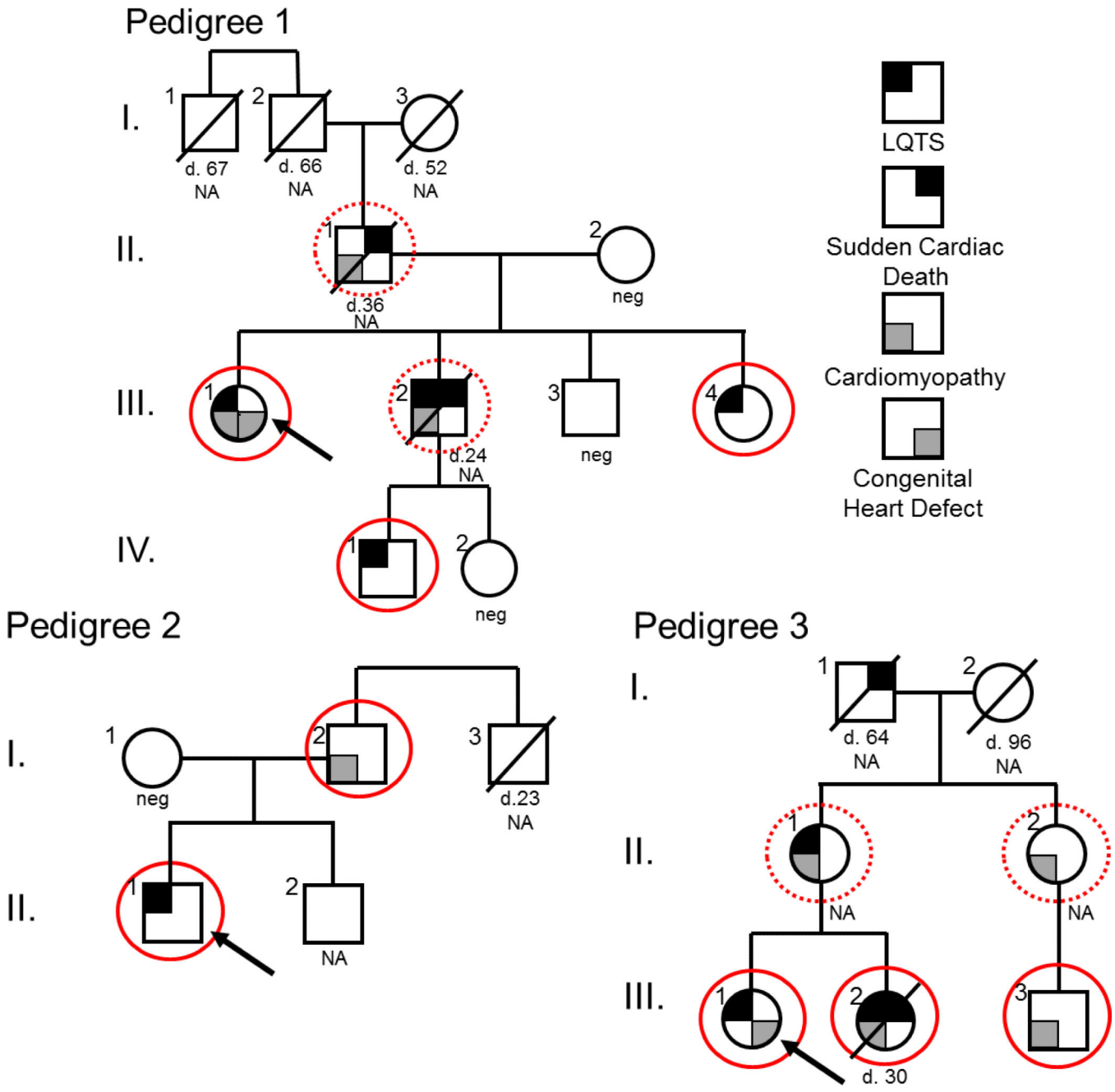

Figure 3.

Pedigrees Harboring p.Arg518Cys/His. The original WES pedigree (pedigree 1), in addition to the pedigrees identified through the cohort analysis (pedigree 2 and 3) show the phenotypic status of each patient (key on right). In addition, each individual with a red circle is p.Arg518Cys/His positive, dotted red circles represent obligate positive p.Arg518Cys/His individuals, those who have been tested and are negative for p.Arg518Cys/His are demarcated with “neg”, and NA represents samples that were not available.

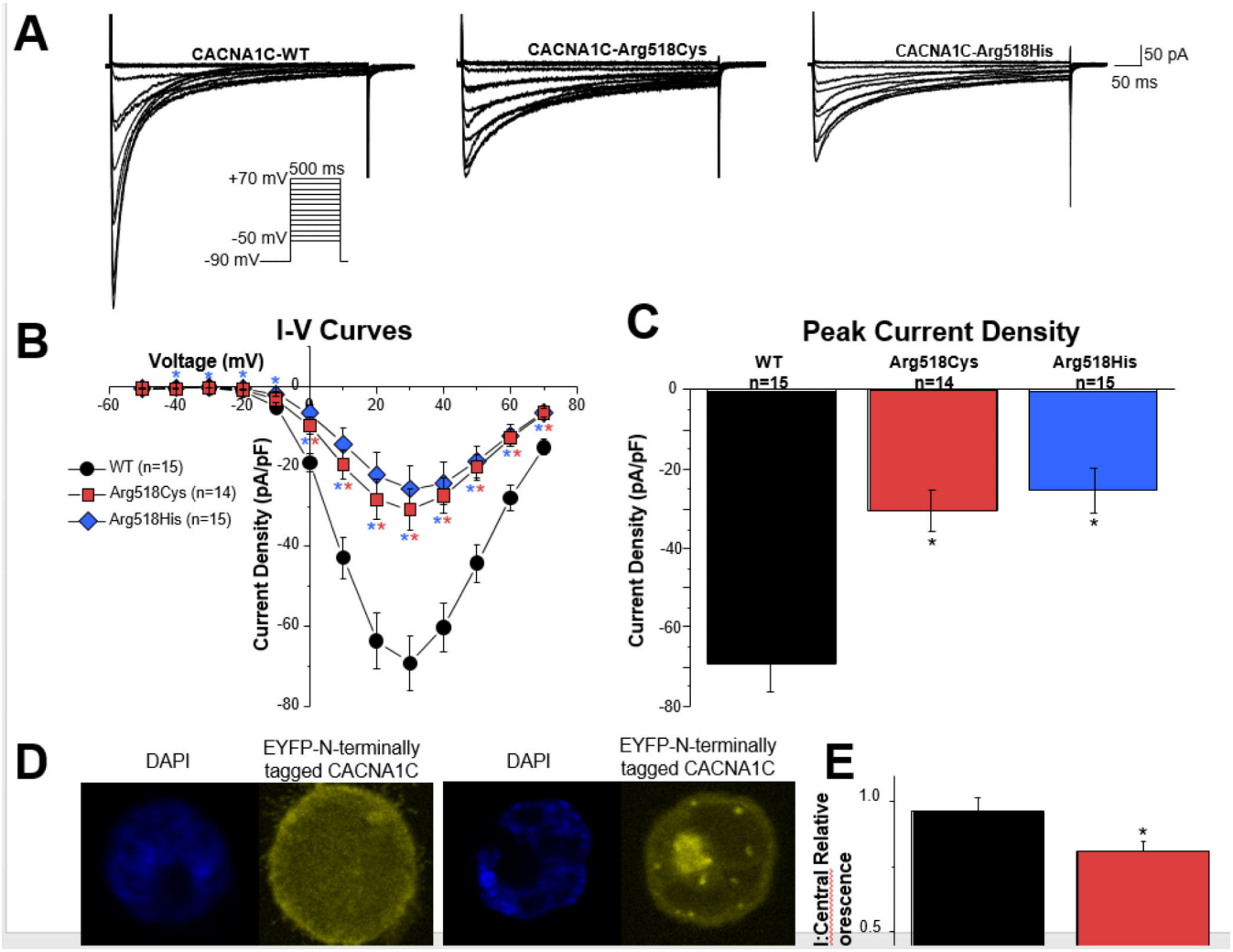

Figure 4.

p.Arg518Cys/His Reduced I_{CaL} Current Density in Heterologous Cells. **(A)** Whole cell I_{CaL} current representative tracings from HEK293 cells expressing WT or mutant p.Arg518Cys/His determined from a holding potential of −90 mV to testing potential of +70 mV in 10 mV increments with 500 ms duration. **(B)** Current-voltage relationship for WT (n=15), and mutant p.Arg518Cys (n=14) and p.Arg518His (n=15) missense mutations. **(C)** Bar graph representing peak current density for WT (n=15), p.Arg518Cys (n=14), and p.Arg518His (n=15). All values represent mean ± SEM. *p<0.05 vs. CACNA1C-WT. **(D)** Confocal studies examining WT and mutant expression of N-terminally tagged CACNA1C with EYFP. The upper left corner of each image represents the DAPI nuclear stain, the upper right corner represents EYFP-CACNA1C, and the lower left corner shows the merged image. **(E)** Bar graph representing the peripheral:central fluorescence of WT (n=10) and p.Arg518Cys (n=10) cells. Bars represent mean ± SEM. *p<0.05 vs. CACNA1C-WT for Student's t-tests; *p<0.05 after ANOVA/Kruskal-Wallis with Dunn's correction for multiple comparisons.

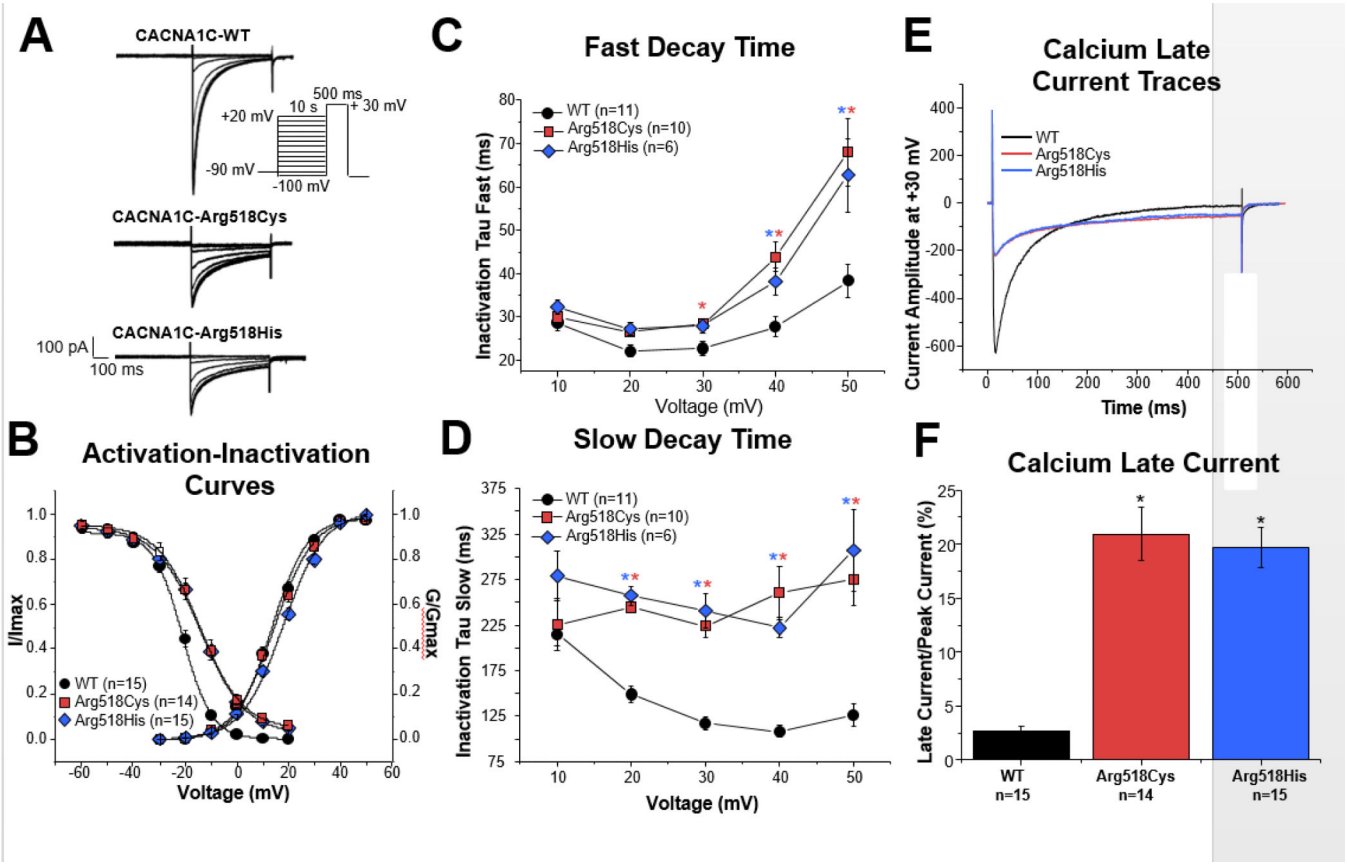

Figure 5.

CACNA1C-Arg518Cys/His Negatively Shifted I_{CaL} $V_{1/2}$ Inactivation. **(A)** Representative tracings of steady-state I_{CaL} inactivation representing WT, p.Arg518Cys, and p.Arg518His determined from a holding potential of −90 mV to pre-pulse of 20 mV in 10 mV increments with 10 s duration followed by a test pulse of 30 mV with 500 ms duration. **(B)** Inactivation curves of I_{CaL} WT (n=15), p.Arg518Cys (n=14), and p.Arg518His (n=15), determined from a holding potential of −90 mV to pre-pulse of 20 mV in 10 mV increments with 10 s duration followed by a test pulse of 30 mV with 500 ms duration. I/Imax represent normalized calcium current fitted with a Boltzmann function. Activation curves of I_{CaL} WT (n=15), p.Arg518Cys (n=14), and p.Arg518His (n=15). G/Gmax represents normalized conductance fitted with a Boltzmann function. **(C)** Inactivation time constants (τ) for the fast phase of I_{CaL} decay time of WT (n=11), p.Arg518Cys (n=10), and p.Arg518His (n=6) as a function of voltage. Time constants for each voltage step were determined by fitting a biexponential function to current decay. **(D)** Inactivation time constants (τ) for the slow phase of I_{CaL} decay time of WT (n=11), p.Arg518Cys (n=10), and p.Arg518His (n=6) as a function of voltage. **(E)** Representative tracings of late current representing WT, p.Arg518Cys, and p.Arg518His measured at the end of 500 ms long depolarization of. **(F)** Normalized late current to peak current shown as percentages in a bar graph for WT, p.Arg518Cys, and p.Arg518His. All values represent mean ± SEM. *p<0.05 vs. CACNA1C-WT for Student's t-tests; *p<0.05 after ANOVA/Kruskal-Wallis with Dunn's correction for multiple comparisons.

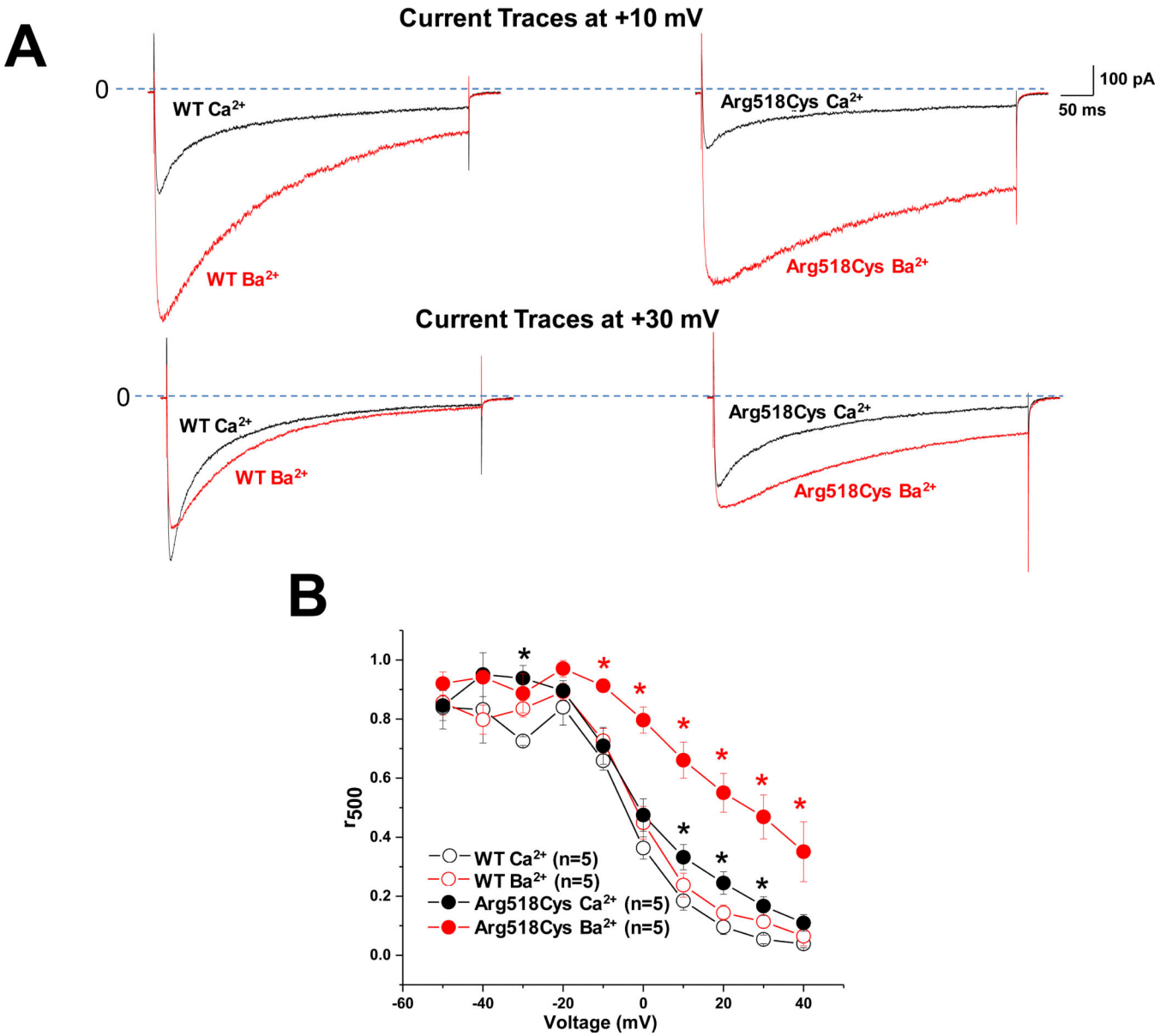

Figure 6.

Deceleration of VDI by p.Arg518Cys-CACNA1C. **(A)** Whole cell I_{Ca} and I_{Ba} current representative tracings from HEK293 cells expressing WT or mutant p.Arg518Cys determined from a holding potential of -90 mV to testing potential of +10 mV and +30 mV with 500 ms duration. **(B)** Voltage-dependent inactivation of I_{Ca} and I_{Ba} currents for WT and p.Arg518Cys channels (n=5 for each group, red *p<0.05 vs. WT I_{Ba}, black *p<0.05 vs. WT I_{Ca}; statisticscompleted for each of the 10 voltages). r_{500} represented fraction of current remaining after 500 ms depolarization normalized to peak current (r500).

Table 1

Patients with LQTS with Personal or Family History of HCM-Like Phenotype

Patient #	Sex	Age at Dx (years)	QTc (ms)	Symptomatic	HCM-Like Phenotype
1*	**M**	**10**	**480**	**No**	**Father with HCM**
2	M	13	493	No	SCD in two cousins with reported increased left ventricular wall thickness on autopsy
3*	**F**	**25**	**558**	**Yes – torsades de pointes during surgery**	**Sister, aunt, and cousin with HCM**
4	F	28	513	Yes – syncope	Cardiomyopathy with septal wall motion abnormalities
5	F	46	493	Yes – cardiac arrest	Postpartum cardiomyopathy

* p.Arg518Cys/His Mutation Positive

Table 2

Summary of Pedigrees 1, 2, and 3

Pedigree	Patient	Symptoms	QTc (ms)	R518 Status
1	I.1	Died unexpectedly at age of 67 – heart attack	NA	NA
1	I.2	Died unexpectedly at age of 66 – heart attack	NA	NA
1	I.3	Died at age of 52 during heart surgery	NA	NA
1	II. 1	SCD at 36 years due to cardiac arrhythmia secondary to primary cardiomyopathy and hypertrophy	NA	Obligate Positive
1 †	II.2	Asymptomatic	NA	Negative
1 * †	**III.1**	**LQTS, VSD, peripartum cardiomyopathy, HCM, 1st degree AV block**	**500**	**Positive**
1	III.2	SCD at 24 years, prolonged QT, autopsy revealed HCM-like phenotype of cardiomegaly and interstitial fibrosis	490	Obligate Positive
1	III.3	Asymptomatic	405	Negative
1 †	III.4	LQTS	491	Positive
1 †	IV.1	LQTS – syncope	522	Positive
1	IV.2	Asymptomatic	NA	Negative
2	I.1	Asymptomatic	NA	Negative
2	I.2	HCM	NA	Positive
2	I.3	Died at 23 years of age during single motor vehicle accident	NA	NA
2 *	**II.1**	**LQTS, sinoatrial node dysfunction**	**480**	**Positive**
2	II.2	Asymptomatic	NA	NA
3	I.1	SCD at 64 years while in the hospital	NA	NA
3	I.2	Asymptomatic	NA	NA
3	II.1	Septal hypertrophy and QT prolongation	NA	Obligate Positive
3	II.2	HCM	NA	Obligate Positive
3 *	**III.1**	**LQTS, cleft mitral valve, ASD, torsades de pointes during surgery, premature atrial complexes**	**500**	**Positive**
3	III.2	SCD at 30 years, previous history of HCM and QT prolongation	NA	Positive
3	III.3	HCM, subaortic stenosis, 1st degree AV block	444	Positive

NA signifies not available

* **Index Cases**

† Whole exome sequenced